Emergence of magnetic topological states in topological insulators doped with magnetic impurities

Minh-Tien Tran
Institute of Research and Development, Duy Tan University, K7/25 Quang Trung, Danang, Vietnam
and Institute of Physics, Vietnam Academy of Science and Technology, 10 Dao Tan, Hanoi, Vietnam

Hong-Son Nguyen
Department of Occupational Safety and Health, Trade Union University, 169 Tay Son, Hanoi, Vietnam

Duc-Anh Le
Faculty of Physics, Hanoi National University of Education,136 Xuan Thuy, Cau Giay, Hanoi, Vietnam
(Received 15 December 2015; revised manuscript received 24 February 2016; published 27 April 2016)

Emergence of the topological invariant and the magnetic moment in topological insulators doped with magnetic impurities is studied based on a mutual cooperation between the spin-orbit coupling of electrons and the spin exchange of these electrons with magnetic impurity moments. The mutual cooperation is realized based on the Kane-Mele model in the presence of magnetic impurities. The topological invariants and the spontaneous magnetization are self-consistently determined within the dynamical mean-field theory. We find different magnetic topological phase transitions, depending on the electron filling. At half filling an antiferromagnetic topological insulator, which exhibits the quantum spin Hall effect, exists in the phase region between the paramagnetic topological insulator and the trivially topological antiferromagnetic insulator. At quarter and three-quarter fillings, a ferromagnetic topological insulator, which exhibits the quantum anomalous Hall effect, occurs in the strong spin-exchange regime.

DOI: 10.1103/PhysRevB.93.155160

I. INTRODUCTION

Recently, the quantum anomalous Hall effect (QAHE) has been observed in topological insulators doped with magnetic impurities [1–3]. It has attracted attention to study the emergence of both topological and magnetic properties in these materials. While the magnetic phase can be described by the Landau phase theory, the topological state cannot. The topological state is a novel concept that is characterized by nontrivial topological invariants which are robust to interactions and disorders [4–7]. Its first realization was found in the quantum Hall effect (QHE) [8–10]. However, this realization requires an external magnetic field that generates the Landau levels. The topological state can also exist in systems without the Landau levels. Haldane first proposed a theoretical model which exhibits the QHE in a periodic lattice [11]. Recently, the Haldane model was experimentally realized by loading ultracold atoms into an optical lattice [12]. Inspired by the Haldane idea, a novel class of topological states, namely, the topological insulator, was discovered [4,5]. Its topological invariant in two-dimensional systems is manifested in the quantum spin Hall effect (QSHE). The topological insulator has also been extended to three-dimensional systems [6,7]. Its topological property is induced by the spin-orbit coupling (SOC) and is characterized generally by the topological invariant number Z_2 [4–7]. In contrast, the spontaneous magnetization is described by an order parameter of the Landau theory. It can act inside the bulk of materials like an external magnetic field that can induce an anomalous Hall effect [13]. The quantized version of the anomalous Hall effect was a long standing problem until its recent discovery in topological insulators doped with magnetic impurities [1–3]. In these materials, the spontaneous magnetization occurs due to the spin exchange (SE) between electrons and magnetic impurities [1–3]. The SOC together with the SE emerge and give rise to the quantization of anomalous Hall effect [1–3]. It is thus desirable to study the mutual cooperation between the SOC and SE as well as their emergence, which possibly causes the QSHE and/or the QAHE.

In this paper, we address the emergence of topological and magnetic properties in topological insulators doped with magnetic impurities. We propose a minimal model that could possibly describe both topological and magnetic properties. The SOC is an essential ingredient for the topological property. It causes a band inversion that induces a nontrivial topological invariant [4–7]. However, the spontaneous magnetization can be induced by different sources, for instance, the SE, the Coulomb interaction, or the superexchange. The QAHE was observed in materials doped with magnetic impurities and the SE between electrons and magnetic impurities is its natural origin [1–3]. Moreover, it does not seem possible that the Coulomb interaction between electrons can induce a topological state with a long-range magnetic order [14–16]. Therefore, in the proposed model, the SE is the other essential ingredient for a long-range magnetic order, which possibly coexists with the topological invariants. A realistic band model with the SE has been theoretically proposed for searching the QAHE in topological insulators [1]. It was studied by a combination of the first-principles calculations for determining the band structure and a mean-field approximation for treating the SE [1]. The QAHE was found in a ferromagnetic (FM) state [1]. However, in the mean-field approximation only a uniform FM order parameter is assumed, and it was treated merely as an input parameter in determining the topology invariant [1]. In this paper we study the mutual cooperation of the SOC and the SE in a self-consistent manner that possibly stabilizes magnetic topological states. We consider a theoretical model, which describes both the SOC and the

SE, namely, the Kane-Mele model [17] with the SE between electrons and magnetic moments. We employ the dynamical mean-field theory (DMFT) [18] to study the emergence of the topological invariant and magnetic moment. The DMFT has been widely used to treat the strong correlations in different complex systems [19]. In particular, it was successfully used to study the magnetically doped materials [20–25]. In contrast to the previous mean-field study [1], in the present study the spontaneous magnetization is self-consistently determined without *a priori* assumption. We find different magnetic topological states and, in particular, a coexistence of the QAHE or of the QSHE with a long-range magnetic order, depending on the electron filling. At half filling, the ground state is antiferromagnetic (AFM), and the spin Hall conductance is quantized in an intermedium regime of the SE, whereas at quarter and three-quarter fillings the ground state is FM, and the charge Hall conductance is quantized, providing strong SE.

The present paper is organized as follows. In Sec. II we propose a model which describes both the SOC of electrons and the SE between electrons and magnetic moments. In that section we also present the application of the DMFT to solve the proposed model. Numerical results of the magnetic topological insulator solutions are presented in Sec. III. Finally, the conclusions are presented in Sec. IV.

II. THE MODEL AND ITS DYNAMICAL MEAN-FIELD THEORY

A minimal model that could describe a magnetic topological insulator would consist of three terms. One term describes the band energy of electrons. The second term that could cause the topological property is the SOC. The last term is essentially the SE between electrons and magnetic moments. For simplicity, explicit magnetic interactions between magnetic moments can be switched off from the model. They are implicitly present in the model through the SE. The model Hamiltonian reads

$$H = -t \sum_{\langle i,j\rangle,\sigma} c^{\dagger}_{i\sigma} c_{j\sigma} + i\lambda \sum_{\langle\langle i,j\rangle\rangle,s,s'} \nu_{ij} c^{\dagger}_{is} \sigma^{z}_{ss'} c_{js'} - J \sum_{i,ss'} \mathbf{S}_i c^{\dagger}_{is} \boldsymbol{\sigma}_{ss'} c_{is'}, \quad (1)$$

where $c^{\dagger}_{i\sigma}$ ($c_{i\sigma}$) is the creation (annihilation) operator for the electron with spin σ at site i. $\langle i,j\rangle$ and $\langle\langle i,j\rangle\rangle$ denote the nearest-neighbor and next-nearest-neighbor sites in the lattice, respectively. t is the hopping parameter for the nearest-neighbor sites. λ is the SOC which involves the spin and direction dependent hopping between next-nearest-neighbor sites. The sign $\nu_{ij} = \pm 1$ depends on the hopping direction as shown in Fig. 1. The honeycomb lattice is chosen, since the SOC in this lattice induces a topological insulator state [17]. $\mathbf{S}_i$ is the spin of the magnetic impurity at site i, and $\boldsymbol{\sigma}$ are the Pauli matrices. J is the SE between electron and magnetic impurity. We consider only the substitutional doping of magnetic impurities, and avoid any interstitial one. When the magnetic impurities are densely doped, we assume that the magnetic impurities occupy every lattice site. We also treat the spin of magnetic impurities classically, as widely used in the studies of materials doped with magnetic impurities [20–25].

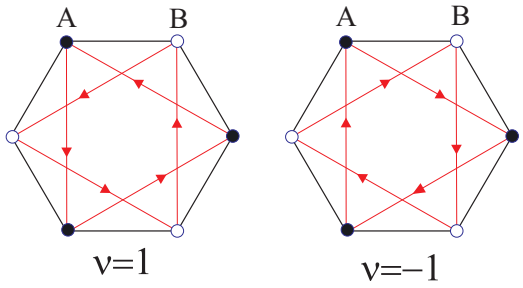

FIG. 1. The sign structure ν_{ij} of the SOC term in the honeycomb lattice.

This consideration excludes any possibility of the Kondo effect [26–29]. Actually, we will only consider the ferromagnetic SE, which blocks the Kondo effect, as confirmed by the quantum Monte Carlo simulations [30]. When the SE is absent ($J = 0$), the proposed model is the Kane-Mele model [17]. This model has, in addition to the time-reversal symmetry, a U(1) symmetry which preserves the z component of spin. This allows us to classify the topological invariant of the insulating state by the spin Chern number [17]. The Kane-Mele model can be viewed as two copies of the Haldane model, in which the insulating state has opposite z components of spin and opposite Chern numbers [11]. This leads to a vanishing of the charge Chern number, but a final integer of the spin Chern number, which yields the QSHE. In the other limit, $\lambda = 0$, the Hamiltonian in Eq. (1) is essentially the double exchange model [23]. It exhibits a magnetic phase transition driven by the SE [20–23]. The double exchange model on frustrated lattices such as the kagome or triangular lattices can also induce the QHE [31,32]. When both the SOC and the SE are present, their mutual cooperation may lead to an emergence of topological and magnetic properties, that possibly causes the QSHE and/or the QAHE.

Before describing the DMFT, we analyze the magnetic structure of the proposed model. The impurity classical spins can be expressed via their azimuthal φ_i and polar θ_i angles:

$$S^x_i = S\cos\varphi_i \sin\theta_i,$$
$$S^y_i = S\sin\varphi_i \sin\theta_i,$$
$$S^z_i = S\cos\theta_i.$$

The SE term in the Hamiltonian in Eq. (1) can be diagonalized by using the unitary transformation

$$\begin{pmatrix} d_{i\uparrow} \\ d_{i\downarrow} \end{pmatrix} = \mathbf{U}^{\dagger}_i \begin{pmatrix} c_{i\uparrow} \\ c_{i\downarrow} \end{pmatrix},$$

where

$$\mathbf{U}_i = \begin{pmatrix} \cos\frac{\theta_i}{2} & -\sin\frac{\theta_i}{2} e^{-i\varphi_i} \\ \sin\frac{\theta_i}{2} e^{i\varphi_i} & \cos\frac{\theta_i}{2} \end{pmatrix}.$$

We obtain the SE term

$$H_{\mathrm{SE}} = -J \sum_{i,ss'} \mathbf{S}_i c^{\dagger}_{is} \boldsymbol{\sigma}_{ss'} c_{is'} = -JS \sum_{i,\sigma} \sigma d^{\dagger}_{i\sigma} d_{i\sigma},$$

where $\sigma = \pm 1$. The SE term is responsible for the spontaneous magnetization. It is expected to occur in the regime $J \gg t,\lambda$. In this regime, only $d_{i\uparrow}$ is relevant to the ground state. The effective Hamiltonian describing the hopping term and the

SOC in the ground state reads [22]

$$H_{\rm eff} = -t\sum_{\langle i,j\rangle}\Omega_{ij}d^{\dagger}_{i\uparrow}d_{j\uparrow} + i\lambda\sum_{\langle\langle i,j\rangle\rangle}\nu_{ij}\widetilde{\Omega}_{ij}d^{\dagger}_{i\uparrow}d_{j\uparrow} + \text{H.c.}, \quad (2)$$

where

$$\Omega_{ij} = \cos\frac{\theta_i}{2}\cos\frac{\theta_j}{2} + \sin\frac{\theta_i}{2}\sin\frac{\theta_j}{2}e^{-i(\varphi_i-\varphi_j)},$$

$$\widetilde{\Omega}_{ij} = \cos\frac{\theta_i}{2}\cos\frac{\theta_j}{2} - \sin\frac{\theta_i}{2}\sin\frac{\theta_j}{2}e^{-i(\varphi_i-\varphi_j)},$$

sometimes referred to as Berry's phases. For simplicity, we will only consider the homogeneous ground state, in which the azimuthal and polar angles of spins do not vary within the two penetrating sublattices. Indeed, in the absence of the SOC, the Monte Carlo simulations reveal the homogeneity of the ground state in the honeycomb lattice [33]. For the homogeneous ground state, the hopping magnitude is maximized when $\theta_i - \theta_j = 0$ or $\pm\pi$ of nearest-neighbor sites. These conditions indicate the spins at nearest-neighbor sites are either parallel or antiparallel, which yields the double exchange mechanism [22,23]. On the other hand, the SOC magnitude is maximized when $\theta_i = 0$ or π, or equivalently, the spin is aligned in the z direction. One can also notice that the SOC term vanishes when $\theta_i = \pi/2$, i.e., when the spin is aligned in the xy plane. In contrast to the frustrated lattices [31,32], both the hopping and SOC terms in the honeycomb lattice do not generate any frustration. From these observations, we conclude that the ground-state energy is minimized when the spins are aligned in the z direction. This indicates the ground state has the U(1) symmetry, which preserves the z component of spin.

We divide the honeycomb lattice into two penetrating sublattices A and B, as shown in Fig. 1. Then we denote $a_{i\sigma}$ ($b_{i\sigma}$) the annihilation operator of the electron when site i belongs to the sublattice A (B). We introduce a four-dimensional spinor

$$\Psi_{\mathbf{k}} = \begin{pmatrix} a_{\mathbf{k}\uparrow} \\ b_{\mathbf{k}\uparrow} \\ a_{\mathbf{k}\downarrow} \\ b_{\mathbf{k}\downarrow} \end{pmatrix},$$

where $a_{\mathbf{k}\sigma}$ and $b_{\mathbf{k}\sigma}$ are the Fourier transforms of $a_{i\sigma}$ and $b_{i\sigma}$, respectively. The magnetic and topological properties will be determined from the single-particle Green's function:

$$\mathbf{G}(\mathbf{k},z) = \{\langle\Psi_{\mathbf{k}}|\Psi^{\dagger}_{\mathbf{k}}\rangle\}_z.$$

The spontaneous magnetization of sublattice A and B is defined as

$$m_A = \frac{1}{2N}\sum_{i,\sigma}\sigma\langle a^{\dagger}_{i\sigma}a_{i\sigma}\rangle,$$

$$m_B = \frac{1}{2N}\sum_{i,\sigma}\sigma\langle b^{\dagger}_{i\sigma}b_{i\sigma}\rangle,$$

where N is the number of sublattice sites. When $m_A = \pm m_B \neq 0$ the ground state is FM or AFM, respectively. Here we consider only the spontaneous magnetization in the z direction, because the ground state has the U(1) symmetry of the z component of spin as we have already analyzed.

The topological property can be determined through the Chern number, which can be calculated by

$$C_\nu = \frac{1}{2\pi}\int d^2k\mathcal{F}^{\nu}_{xy}, \quad (3)$$

where $\mathcal{F}^{\nu}_{ij} = \partial_i\mathcal{A}^{\nu}_j - \partial_j\mathcal{A}^{\nu}_i, \mathcal{A}^{\nu}_i = -i\langle\mathbf{k}\nu|\partial_{k_i}|\mathbf{k}\nu\rangle$, and $|\mathbf{k}\nu\rangle$ is the orthonormalized eigenstate of matrix $\mathbf{G}^{-1}(\mathbf{k},i0)$, corresponding to the eigenvalue $E_\nu(\mathbf{k})$ [34]. The charge Chern number $C_c = \sum_\nu{}' C_\nu$, where this sum is taken over ν with positive eigenvalue $E_\nu(\mathbf{k}) > 0$. The spin Chern number $C_s = \sum_\nu{}' \sigma_\nu C_\nu$, where σ_ν is the spin of the eigenstate $|\mathbf{k}\nu\rangle$. Note that these Chern numbers are well defined only in the insulating state, since it requires a gap separation between the positive and negative eigenvalues. In numerical calculations we can use the efficient method of discretization of the Brillouin zone to calculate the Chern number in Eq. (3) [35]. In the topological insulator, the Hall conductance is e^2C_c/h, while the spin one is e^2C_s/h. Without the SE interaction, $\mathbf{G}^{-1}(\mathbf{k},i0) = -\mathbf{H}_0(\mathbf{k})$, where

$$\mathbf{H}_0(\mathbf{k}) = \begin{pmatrix} \mathbf{h}_\uparrow(\mathbf{k}) & 0 \\ 0 & \mathbf{h}_\downarrow(\mathbf{k}) \end{pmatrix} \quad (4)$$

is the noninteraction Bloch Hamiltonian, and

$$\mathbf{h}_\sigma(\mathbf{k}) = \begin{pmatrix} \sigma\lambda\xi_{\mathbf{k}} & -t\gamma_{\mathbf{k}} \\ -t\gamma^*_{\mathbf{k}} & -\sigma\lambda\xi_{\mathbf{k}} \end{pmatrix}.$$

Here we have used the notations $\gamma_{\mathbf{k}} = \sum_\delta e^{i\mathbf{k}\cdot\mathbf{r}_\delta}, \xi_{\mathbf{k}} = i\sum_\eta \nu_\eta e^{i\mathbf{k}\cdot\mathbf{r}_\eta}$, where δ and η denote nearest-neighbor and next-nearest-neighbor sites of a given site in the honeycomb lattice, respectively. The noninteraction Bloch Hamiltonian has two doubly degenerate bands. The SOC opens a band gap and induces an integer spin Chern number at half filling [17]. One can imagine $-\mathbf{G}^{-1}(\mathbf{k},i0)$ as an effective Bloch Hamiltonian, which determines the Chern number for interaction cases.

The proposed model in Eq. (1) can be solved by various methods, which include both mean-field and dynamical mean-field approximations as well as the exact diagonalization and Monte Carlo simulations. The exact diagonalization and the Monte Carlo simulations give the exact result, but they are applicable only for small clusters and admit the finite-size effect. The mean-field and dynamical mean-field approximations are valid in the thermodynamical limit. In contrast to the mean-field approximation, the DMFT treats the local correlations exactly [19]. Without the SOC ($\lambda = 0$), the phase diagram obtained by the DMFT agrees well with the one obtained by the Monte Carlo simulations [21,22]. The mean-field approximation sometimes produces an artifact, for instance, the canted state found by the de Gennes mean-field approximation is not supported by the Monte Carlo simulations [21,36]. The DMFT can serve as a complementary method to finite cluster calculations such as the Monte Carlo simulations. In this paper we use the DMFT. Within the DMFT, the self-energy depends only on frequency. It is exact in the infinite-dimension limit, but in two-dimensional systems it is just an approximation. This approximation neglects nonlocal correlations. In honeycomb lattice, the DMFT overestimates the semimetal-insulator transition, but it is still capable of detecting the insulating or magnetic states [37–40]. For the ferromagnetic Kondo model, the DMFT reproduces well the

Monte Carlo simulation results [21,22]. Within the DMFT the Dyson equation for the Green's function reads

$$\mathbf{G}(\mathbf{k},z) = [z - \mathbf{H}_0(\mathbf{k}) - \mathbf{\Sigma}(z)]^{-1}, \tag{5}$$

where $\mathbf{\Sigma}(z)$ is the self-energy. Actually, $\mathbf{\Sigma}(z)$ is a 4×4 diagonal matrix. The local approximation of the self-energy does not mix the two spin sectors of the effective Bloch Hamiltonian $-\mathbf{G}^{-1}(\mathbf{k},i0)$. For the topological invariants, the self-energy just shifts the bands of the effective Bloch Hamiltonian, that can cause topological transitions. The self-energy can be determined by solving of an effective single site coupled with a dynamical mean field. The dynamical mean field can be represented by a Green's function, which serves as the bare Green's function of the effective single site. It connects with the local Green's function and the self-energy via the Dyson equation

$$\mathcal{G}^{-1}_{a\sigma}(z) = G^{-1}_{a\sigma}(z) + \Sigma_{a\sigma}(z), \tag{6}$$

where a denotes the sublattice notation of the single site. $G_{a\sigma}(z) = \sum_{\mathbf{k}} G_{a\sigma}(\mathbf{k},z)/N$ is the local Green's function. The action of the effective single site of sublattice $a = A,B$ is

$$\begin{aligned}\mathcal{S}_a = &-\sum_s \int_0^\beta \int_0^\beta d\tau d\tau' \Psi^\dagger_{as}(\tau)\mathcal{G}^{-1}_{as}(\tau-\tau')\Psi_{as}(\tau') \\ &- J\sum_{\alpha ss'} \int_0^\beta d\tau S^\alpha(\tau)\Psi^\dagger_{as}(\tau)\sigma^\alpha_{ss'}\Psi_{as'}(\tau).\end{aligned} \tag{7}$$

For classical impurity spin $\mathbf{S}$, we can exactly solve the effective single-site action. One can find the partition function of the effective single site:

$$\mathcal{Z}_a = \int_0^{2\pi} d\varphi \int_0^{\pi} d\theta \sin\theta e^{-S_a(\varphi,\theta)}, \tag{8}$$

where

$$\begin{aligned}&S_a(\varphi,\theta) \\ &= -\sum_n \ln\left\{\prod_s \left[\mathcal{G}^{-1}_{as}(i\omega_n) + sJS\cos\theta\right] - (JS)^2\sin^2\theta\right\},\end{aligned}$$

and ω_n is the Matsubara frequency. The single-site Green's function can be calculated from the partition function:

$$\begin{aligned}&\langle\langle \Psi_{a\sigma}|\Psi^\dagger_{a\sigma}\rangle\rangle_{i\omega_n} \\ &= \frac{1}{\mathcal{Z}_a}\frac{\delta\mathcal{Z}_a}{\delta\mathcal{G}^{-1}_{a\sigma}(i\omega_n)} \\ &= \frac{1}{\mathcal{Z}_a}\int_0^{2\pi} d\varphi \int_0^{\pi} d\theta \sin\theta e^{-S(\varphi,\theta)} \\ &\quad \times\left[\mathcal{G}^{-1}_{a,-\sigma}(i\omega_n) - \sigma JS\cos\theta\right] \Big/ \\ &\quad \left\{\prod_s \left[\mathcal{G}^{-1}_{as}(i\omega_n) + sJS\cos\theta\right] - (JS)^2\sin^2\theta\right\}.\end{aligned} \tag{9}$$

Using again the Dyson equation in Eq. (6) we can determine the self-energy, once the Green's function of the single site is computed by Eq. (9). So far, we have obtained a complete system of equations which self-consistently determine the self-energy and the Green's function. This system of DMFT equations can be solved numerically by simple iterations [19].

III. EMERGENCE OF MAGNETIC TOPOLOGICAL STATES

In numerical calculations, we take $t = 1$ as the energy unit. At zero temperature, we use a fine mesh for frequency, and the mesh size serves as a fictitious temperature. Actually, we take the mesh size $2\pi T$ with $T = 0.01$ in numerical calculations. First, we find out the conditions for the existence of the insulating state, because in the model under consideration only the insulator can possibly exhibit the topological properties. In Fig. 2 we plot the electron filling n and the sublattice magnetization m_A, m_B as a function of the chemical potential μ for increasing values of the SE at a given SOC. Whenever the μ dependence of the electron filling n exhibits a plateau, it indicates an insulating state. For SE $JS = 0$, the ground state is the insulator at half filling $n = 1$. Since $m_A = m_B = 0$, this insulator is paramagnetic (PM), as expected. Weak SEs do not change this ground state. However, when the SE is larger than a certain value, a spontaneous magnetization occurs, $m_A = -m_B \neq 0$, at half filling, and it indicates an AFM insulating state. With further increasing SE, additional insulating states appear at quarter ($n = 0.5$) and three-quarter

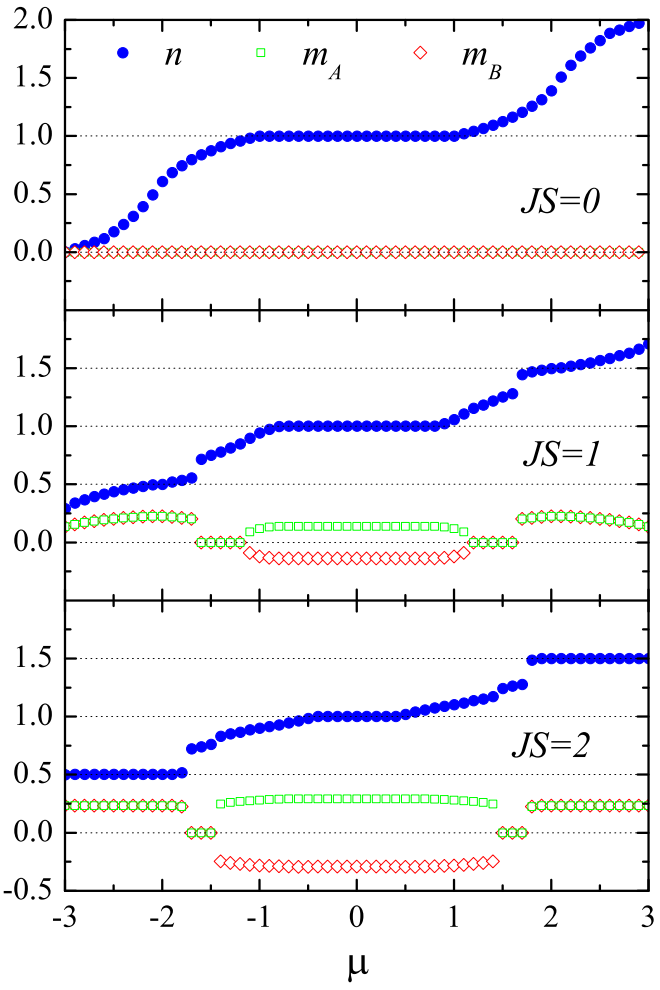

FIG. 2. The electron filling n and the sublattice magnetization m_A, m_B via the chemical potential μ for different values of the SE at fixed SOC $\lambda = 0.5$. The horizontal dotted lines indicate fillings $n = 0.5, 1.0, 1.5$.

($n = 1.5$) fillings. These insulating states are FM due to $m_A = m_B \neq 0$. Actually, the quarter and three-quarter fillings are equivalent via the particle-hole symmetry. So far, we have observed the insulating state only at half, quarter, and three-quarter fillings. For other fillings the ground state is metallic or phase separation. The phase separation appears at the discontinuities of $n(\mu)$. It occurs between PM and FM (or AFM) phases. At half filling the SE drives the ground state from PM insulator to AFM insulator, whereas at quarter and three-quarter fillings it drives the ground state from PM metal to FM metal, and then to FM insulator, as shown in Fig. 2. In materials doped with magnetic impurities such as the colossal magnetoresistance materials or diluted magnetic semiconductors the spontaneous magnetization is induced by the SE through the double exchange mechanism [22,23]. However, in the insulator there are no mediated itinerant electrons, hence the double exchange cannot be realized. Actually, the spontaneous magnetization in the insulating states can also be generated by direct coupling between the magnetic moment and electron spin through the van Vleck mechanism [1]. Such direct coupling is possible because the SOC can connect the conduction and the valence bands [1]. Without the SOC, the spontaneous magnetization hardly exists in the insulating state. The SOC is an essential source that maintains the spontaneous magnetization in the insulating state. From the SOC emerge the topology and magnetism of the system. In contrast to the mean-field approximation [1], the spontaneous magnetization within the DMFT is self-consistently determined, and it can be PM, AFM, or FM. Since within the considered model nontrivial topological invariants can only exist in the insulating state, we will consider the half- and quarter- (three-quarter-) filling cases separately.

A. Antiferromagnetic topological insulator

In this subsection we consider the half-filling case in detail. In Fig. 3 we plot the sublattice magnetizations m_A,m_B and the spin Chern number C_s at a given value of the SOC. We always obtain $m_A = -m_B$ at half filling. For weak SEs the ground state is PM. It becomes AFM when the SE is larger than a certain value J_M. In contrast to the Mott insulator [41], the self-energy $\mathbf{\Sigma}(i\omega)$ at half filling does not diverge in the limit $\omega \to 0$, and we can calculate the Chern number by the formula in Eq. (3). The charge Chern number always vanishes at half filling. Figure 3 also shows that the spin Chern number $C_s = 1$ until a certain value J_C of the SE. This means that the topological invariant is nontrivial for $J < J_C$. We always obtain $J_M < J_C$. Therefore, when $J_M < J < J_C$, the ground state is AFM and it has $C_s = 1$. This is an emergence of the magnetic topological insulating state. Indeed, the effective Bloch Hamiltonian $-\mathbf{G}^{-1}(\mathbf{k},i0)$, which determines the Chern number for the interaction case, can be viewed as two copies of the Haldane model with opposite phases [11]. When its two lowest bands with opposite spins are occupied, i.e., the negative eigenvalues of $-\mathbf{G}^{-1}(\mathbf{k},i0)$, they have opposite Chern numbers, therefore the charge Chern number vanishes, while the spin Chern number is a finite integer. On the other hand, the SE induces the spontaneous AFM magnetization. This AFM magnetization can effectively play as an additional molecular magnetic field which acts back to electrons. This effective action of the AFM magnetization is similar to the staggered field in the Haldane model [11]. With increasing SE, the AFM magnetization increases. As a consequence, when $J > J_C$, the Chern number of the corresponding Haldane model vanishes, since the staggered field is larger than the band gap opened by the SOC [11]. This leads the ground state to be topologically trivial. However, the spin Chern number can be a finite integer, providing the staggered field is smaller than the threshold value. The spin Chern number $C_s = 1$ yields the QSHE.

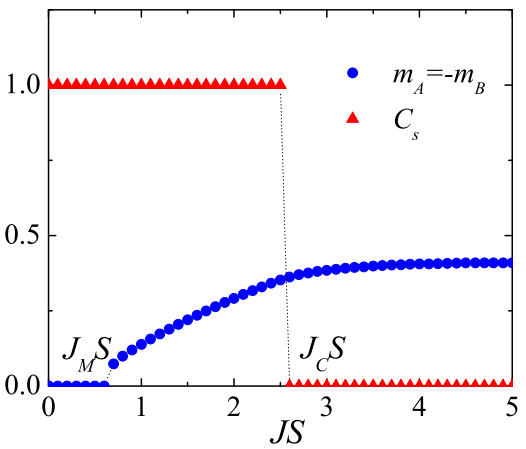

FIG. 3. The sublattice magnetization $m_A = -m_B$ and the spin Chern number C_s at half filling and fixed SOC $\lambda = 0.5$.

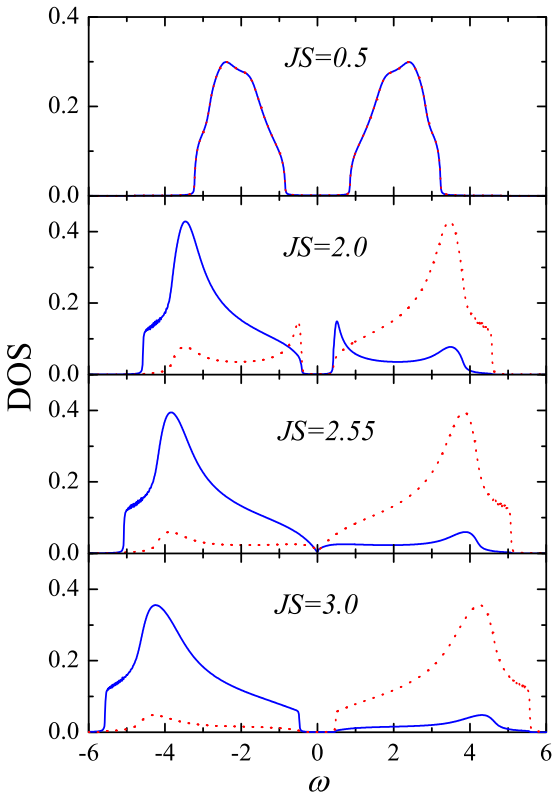

FIG. 4. The sublattice DOS for up-spin (blue solid line) and down-spin (red dotted line) at half filling and fixed SOC $\lambda = 0.5$.

In Fig. 4 we plot the density of states (DOS) for each electron spin component at half filling. It shows an evolution of the DOS when the SE increases. At half filling the DOS clearly displays a gap at the chemical potential level, except at the boundary between the topological AFM insulator and the topologically trivial AFM insulator. At the boundary, the DOS exhibits a semimetal behavior. It indicates a gap closing when the system crosses the phase transition from the topological AFM insulator to the topologically trivial AFM insulator. Actually, this behavior is a result of the gapless edge states, which occur at the boundary of two insulating states with different topological invariants [6,7]. In the topological insulating state, while the SOC maintains the band gap, the spontaneous AFM magnetization reduces the band gap (see also Fig. 2). When these two counteractions are balanced, the gap vanishes and this yields the phase transition from topological AFM insulator to a topologically trivial one. In the topologically trivial AFM insulator, both SOC and the spontaneous AFM magnetization increase the band gap. In contrast to the FM magnetization in the QAHE, the AFM magnetization does not induce the QSHE, because the QSHE already occurs in the PM topological state. It rather destroys the QSHE. However, the AFM long-range order can coexist with the QSHE, providing it is not strong enough. In the strong SE regime, the ground state is topologically trivial AFM.

We summarize the finding results at half filling in a phase diagram, which is plotted in Fig. 5. The AFM topological insulator occurs in the phase region between the PM topological insulator and the topologically trivial AFM insulator. It exhibits the QSHE. Actually, the QSHE is also present in the PM topological insulating state. Note that in the line of $\lambda = 0$ the ground state is metallic, and the AFM magnetization occurs due to the double exchange mechanism [22,23].

B. Ferromagnetic topological insulator

Since the quarter and three-quarter fillings are equivalent through the particle-hole symmetry, in this subsection we only consider the quarter-filling case. As we have previously discussed, at quarter filling the SE drives the ground state from PM to FM metal, and then to the FM insulator. These phase transitions are again confirmed by considering the dependence of the sublattice magnetizations and the band gap on the SE strength. In Fig. 6 we plot the the sublattice magnetizations and the band gap via the SE at fixed SOC. The band gap is determined by the width of the plateau, which occurs in the line $n(\mu)$ (see Fig. 2). At quarter filling, we always obtain $m_A = m_B$. The FM state occurs when the SE is larger than a certain value. The band gap is opened only in the strong SE regime. Therefore, the FM insulating state occurs in the strong SE regime. In Fig. 7 we also plot the DOS for each spin component at quarter filling and fixed SOC. This figure shows an evolution of the DOS when the SE increases. In contrast to the half-filling case, at quarter filling the chemical potential does not lie inside the band gap, but in the lower band. Therefore, for weak SEs, the ground state is metallic. The SE shifts the DOS of the down-spin component, that causes the FM spontaneous magnetization. With further increasing of SE, a gap is opened at the position of the chemical potential and it separates the lowest occupied band. This is indeed the FM insulating state. Since the Chern number is well defined only in the insulating state, we compute it only in the FM insulating state. It turns out only the lowest band of the effective Bloch Hamiltonian $-\mathbf{G}^{-1}(\mathbf{k},i0)$ is occupied, i.e., the smallest negative eigenvalue of $-\mathbf{G}^{-1}(\mathbf{k},i0)$, and it has the Chern number $C_c = 1$. This indicates that the FM insulator is topological and it exhibits the QAHE. Actually, one can imagine the FM magnetization as an external magnetic field, which acts back on electrons. A topological analysis of the Kane-Mele model in the presence of a uniform magnetic field shows the QSHE for weak magnetic fields and the QAHE for strong ones [42]. The finding QAHE at quarter filling is in agreement with this analysis. However, in contrast, we do not observe any QSHE for weak SEs at quarter filling. This happens because weak SEs are not strong enough to open a gap at the chemical potential position. The QAHE is clearly a consequence of the mutual cooperation of the SOC and the SE. In contrast to the half-filling case, the FM magnetization at quarter filling maintains the QAHE. Without it the QAHE cannot exist.

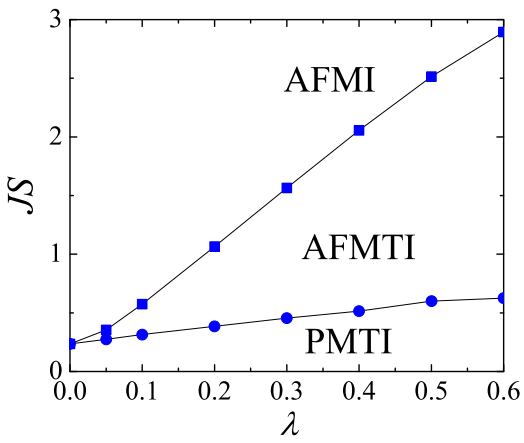

FIG. 5. Phase diagram of the half-filling case. The abbreviations AFMI, AFMTI, and PMTI denote the topologically trivial AFM insulator, AFM topological insulator, and PM topological insulator, respectively.

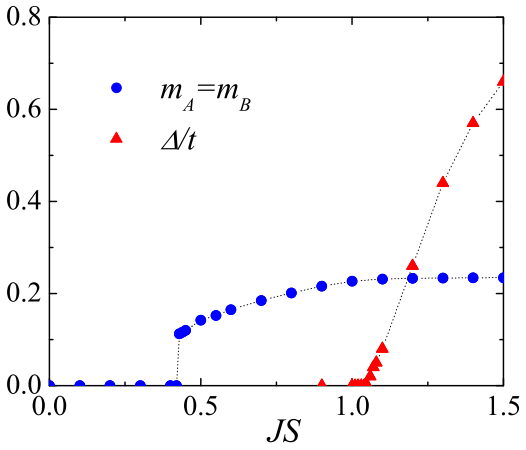

FIG. 6. The sublattice magnetization $m_A = m_B$ and the band gap Δ at quarter filling and fixed SOC $\lambda = 0.5$.

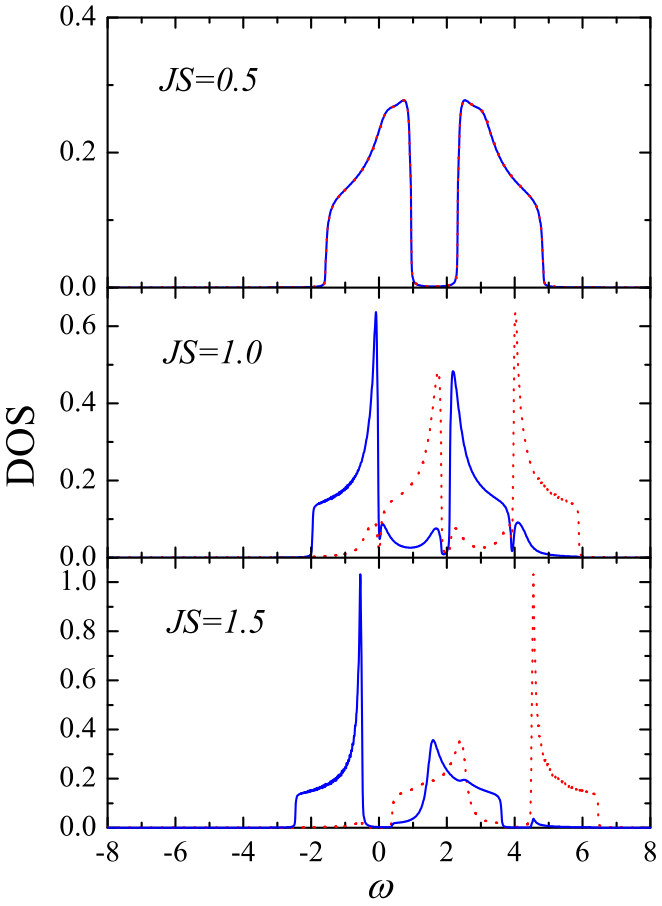

FIG. 7. The sublattice DOS for up-spin (blue solid line) and down-spin (red dotted line) at quarter filling and fixed SOC $\lambda = 0.5$.

We summarize the finding results at quarter filling in a phase diagram, which is plotted Fig. 8. The FM topological insulator, which exhibits the QAHE, occurs only the strong SE regime. When the SOC is absent (i.e., $\lambda = 0$), there is no insulating state at quarter filling. The SE alone drives the phase transition only from the PM to FM metals.

IV. CONCLUSION

In this paper we have studied the emergence of magnetic topological states in the Kane-Mele model in the presence of magnetic impurities. The emergence appears as a result of the mutual cooperation of the SOC and the SE. The insulating states are observed only at half, quarter, and three-quarter fillings. The SOC essentially maintains the spontaneous magnetization in the insulating states. It also favors the magnetization in the z direction, that the ground state preserves the U(1) symmetry of the z component of spin. At half filling, the SE drives the ground state from the PM topological insulator to AFM topological insulator, and then to topologically trivial AFM. Both PM and AFM topological insulators exhibit the QSHE. The AFM topological insulator is another example besides the topological superconductors, in which both long-range order and topological invariant coexist [6,7]. We notice that the studies of the Kane-Mele model with the local Coulomb interaction do not detect the coexistence of the AFM long-range order and topological invariant [14–16]. At quarter and three-quarter fillings, the FM topological insulator, which exhibits the QAHE, occurs in the strong SE regime. However, in our study the magnetic impurities are regularly doped into the lattice. In realistic materials, which exhibit the QAHE such as the Cr-doped $Bi_2(Se_xTe_{1-x})_3$, the magnetic impurities are randomly doped [2,3]. We leave this problem for further studies.

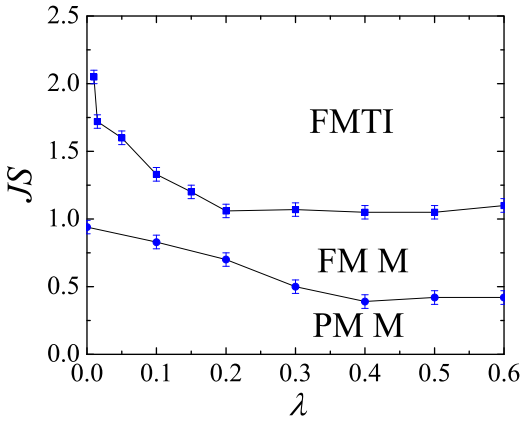

FIG. 8. Phase diagram of the quarter-filling case. The abbreviations FMTI, FM M, and PM M denote the FM topological insulator, FM metal, and PM metal, respectively.

ACKNOWLEDGMENT

This research is funded by the Vietnam National Foundation for Science and Technology Development (NAFOSTED) under Grant No. 103.01-2014.09.

[1] R. Yu, W. Zhang, H.-J. Zhang, S.-C. Zhang, X. Dai, and Z. Fang, Science **329**, 61 (2010).
[2] C.-Z. Chang, J. Zhang, X. Feng, J. Shen, Z. Zhang, M. Guo, K. Li, Y. Ou, P. Wei, L.-L. Wang, Z.-Q. Ji, Y. Feng, S. Ji, X. Chen, J. Jia, X. Dai, Z. Fang, S.-C. Zhang, K. He, Y. Wang, L. Lu, X.-C. Ma, and Q.-K. Xue, Science **340**, 167 (2013).
[3] K. He, Y. Wang, and Q.-K. Xue, Natl. Sci. Rev. **1**, 38 (2014).
[4] B. A. Bernevig, T. L. Hughes, and S.-C. Zhang, Science **314**, 1757 (2006).
[5] M. König, S. Wiedmann, C. Brüne, A. Roth, H. Buhmann, L. W. Molenkamp, X. L. Qi, and S. C. Zhang, Science **318**, 766 (2007).
[6] M. Z. Hassan and C. L. Kane, Rev. Mod. Phys. **82**, 3045 (2010).
[7] X. L. Qi and S. C. Zhang, Rev. Mod. Phys. **83**, 1057 (2011).
[8] K. v. Klitzing, G. Dorda, and M. Pepper, Phys. Rev. Lett. **45**, 494 (1980).
[9] D. C. Tsui, H. L. Stormer, and A. C. Gossard, Phys. Rev. Lett. **48**, 1559 (1982).

[10] D. J. Thouless, M. Kohmoto, M. P. Nightingale, and M. den Nijs, Phys. Rev. Lett. **49**, 405 (1982).
[11] F. D. M. Haldane, Phys. Rev. Lett. **61**, 2015 (1988).
[12] G. Jotzu, M. Messer, R. Desbuquois, M. Lebrat, T. Uehlinger, D. Greif, and T. Esslinger, Nature (London) **515**, 237 (2014).
[13] N. Nagaosa, J. Sinova, S. Onoda, A. H. MacDonald, and N. P. Ong, Rev. Mod. Phys. **82**, 1539 (2010).
[14] S. Rachel and K. Le Hur, Phys. Rev. B **82**, 075106 (2010).
[15] M. Hohenadler, Z. Y. Meng, T. C. Lang, S. Wessel, A. Muramatsu, and F. F. Assaad, Phys. Rev. B **85**, 115132 (2012).
[16] M. Hohenadler and F. F. Assaad, J. Phys.: Condens. Matter **25**, 143201 (2013).
[17] C. L. Kane and E. J. Mele, Phys. Rev. Lett. **95**, 226801 (2005).
[18] W. Metzner and D. Vollhardt, Phys. Rev. Lett. **62**, 324 (1989).
[19] A. Georges, G. Kotliar, W. Krauth, and M. J. Rozenberg, Rev. Mod. Phys. **68**, 13 (1996).
[20] N. Furukawa, J. Phys. Soc. Jpn. **63**, 3214 (1994); **64**, 2754 (1995); **65**, 1174 (1996).
[21] S. Yunoki, J. Hu, A. L. Malvezzi, A. Moreo, N. Furukawa, and E. Dagotto, Phys. Rev. Lett. **80**, 845 (1998).
[22] E. Dagotto, *Nanoscale Phase Separation and Colossal Magnetoresistance*, Springer Series in Solid-State Sciences Vol. 136 (Springer, New York, 2003).
[23] C. Zener, Phys. Rev. **82**, 403 (1951).
[24] Tran Minh-Tien, Phys. Rev. B **67**, 144404 (2003).
[25] Van-Nham Phan and Minh-Tien Tran, Phys. Rev. B **72**, 214418 (2005).
[26] X.-Y. Feng, J. Dai, C.-H. Chung, and Q. Si, Phys. Rev. Lett. **111**, 016402 (2013).
[27] Y. Zhong, Y.-F. Wang, H.-T. Lu, and H.-G. Luo, Phys. Rev. B **88**, 235111 (2013).
[28] Minh-Tien Tran and Ki-Seok Kim, Phys. Rev. B **82**, 155142 (2010).
[29] Minh-Tien Tran, T. Takimoto, and K.-S. Kim, Phys. Rev. B **85**, 125128 (2012).
[30] S. Capponi and F. F. Assaad, Phys. Rev. B **63**, 155114 (2001).
[31] K. Ohgushi, S. Murakami, and N. Nagaosa, Phys. Rev. B **62**, R6065 (2000).
[32] A. Rahmani, R. A. Muniz, and I. Martin, Phys. Rev. X **3**, 031008 (2013).
[33] J. W. F. Venderbos, M. Daghofer, J. van den Brink, and S. Kumar, Phys. Rev. Lett. **107**, 076405 (2011).
[34] Z. Wang and S.-C. Zhang, Phys. Rev. X **2**, 031008 (2012).
[35] T. Fukui, Y. Hatsugai, and H. Suzuki, J. Phys. Soc. Jpn. **74**, 1674 (2005).
[36] P. G. de Gennes, Phys. Rev. **118**, 141 (1960).
[37] S. Sorella and E. Tosatti, Europhys. Lett. **19**, 699 (1992).
[38] M.-T. Tran and K. Kuroki, Phys. Rev. B **79**, 125125 (2009).
[39] W. Wu, Y.-H. Chen, H.-S. Tao, N.-H. Tong, and W.-M. Liu, Phys. Rev. B **82**, 245102 (2010).
[40] S. Sorella, Y. Otsuka, and S. Yunoki, Sci. Rep. **2**, 992 (2012).
[41] Hong-Son Nguyen and Minh-Tien Tran, Phys. Rev. B **88**, 165132 (2013).
[42] Y. Yang, Z. Xu, L. Sheng, B. Wang, D. Y. Xing, and D. N. Sheng, Phys. Rev. Lett. **107**, 066602 (2011).